HHS Public Access

Author manuscript

Nanomedicine. Author manuscript; available in PMC 2015 October 29.

Published in final edited form as:

Nanomedicine. 2015 July ; 11(5): 1039–1046. doi:10.1016/j.nano.2015.02.021.

Prednisolone-containing liposomes accumulate in human atherosclerotic macrophages upon intravenous administration

Fleur M. van der Valk, M.D.[a,1], **Diederik F. van Wijk**[a,1], **Mark E. Lobatto**[a], **Hein J. Verberne**[b], **Gert Storm**[c,h], **Martine C.M. Willems**[d], **Dink A. Legemate**[d], **Aart J. Nederveen**[e], **Claudia Calcagno**[f], **Venkatesh Mani**[f], **Sarayu Ramachandran**[f], **Maarten P.M. Paridaans**[f], **Maarten J. Otten**[f], **Geesje M. Dallinga-Thie**[a], **Zahi A. Fayad**[f], **Max Nieuwdorp**[a], **Dominik M. Schulte**[a,g], **Josbert M. Metselaar**[h], **Willem J.M. Mulder**[a,f], and **Erik S. Stroes, M.D., Ph.D.**[a,*]

Fleur M. van der Valk: f.m.valkvander@amc.nl; Diederik F. van Wijk: d.f.vanwijk@amc.nl; Mark E. Lobatto: m.e.lobatto@gmail.com; Hein J. Verberne: h.j.verberne@amc.nl; Gert Storm: g.storm@uu.nl; Martine C.M. Willems: w.c.willems@amc.nl; Dink A. Legemate: d.a.legemate@amc.nl; Aart J. Nederveen: a.j.nederveen@amc.nl; Claudia Calcagno: claudia.calcagno@mssm.edu; Venkatesh Mani: venkatesh.mani@mssm.edu; Sarayu Ramachandran: sarayu.ramachandran@mssm.edu; Maarten P.M. Paridaans: mpmparidaans@gmail.com; Maarten J. Otten: maartenjotten@gmail.com; Geesje M. Dallinga-Thie: g.m.dallinga@amc.nl; Zahi A. Fayad: zahi.fayad@mssm.edu; Max Nieuwdorp: m.nieuwdorp@amc.nl; Dominik M. Schulte: dominik.schulte@uksh.de; Josbert M. Metselaar: bart@enceladus.nl; Willem J.M. Mulder: wjmmulder@gmail.com; Erik S. Stroes: e.s.stroes@amc.nl

[a]Department of Vascular Medicine, AMC, Amsterdam, The Netherlands [b]Department of Nuclear Medicine, AMC, Amsterdam, The Netherlands [c]Institute for Pharmaceutical Sciences UU, Utrecht, The Netherlands [d]Department of Vascular Surgery, AMC, Amsterdam, The Netherlands [e]Department of Radiology, AMC, Amsterdam, The Netherlands [f]Translational and Molecular Imaging Institute, Icahn School of Medicine at Mount Sinai, New York, NY, USA [g]Department of Internal Medicine I, UKSH, Kiel, Germany [h]Department of Targeted Therapeutics, MIRA Institute UT, Enschede, The Netherlands

Abstract

Drug delivery to atherosclerotic plaques via liposomal nanoparticles may improve therapeutic agents' risk–benefit ratios. Our paper details the first clinical studies of a liposomal nanoparticle encapsulating prednisolone (LN-PLP) in atherosclerosis. First, PLP's liposomal encapsulation improved its pharmacokinetic profile in humans (n = 13) as attested by an increased plasma half-life of 63 h (LN-PLP 1.5 mg/kg). Second, intravenously infused LN-PLP appeared in 75% of the macrophages isolated from iliofemoral plaques of patients (n = 14) referred for vascular surgery in a randomized, placebo-controlled trial. LN-PLP treatment did however not reduce arterial wall permeability or inflammation in patients with atherosclerotic disease (n = 30), as assessed by multimodal imaging in a subsequent randomized, placebo-controlled study. In conclusion, we successfully delivered a long-circulating nanoparticle to atherosclerotic plaque macrophages in patients, whereas prednisolone accumulation in atherosclerotic lesions had no anti-inflammatory effect. Nonetheless, the present study provides guidance for development and imaging-assisted evaluation of future nanomedicine in atherosclerosis.

[*]Corresponding author at: Academic Medical Center, Department of Vascular Medicine, Amsterdam, the Netherlands.

[1]Authors contributed equally.

These other authors declare that they have no competing interests. All other authors declare that they have no conflict of interest and no relationships with industry relevant to this study.

Keywords

Atherosclerosis; Nanomedicine; Glucocorticoids; Macrophages

Because inflammation plays a pivotal role in atherosclerotic plaque development,[1] novel anti-inflammatory strategies[2] are expected to complement and improve existing therapeutic regimens. Delivering drugs via nanocarriers may reduce atherosclerotic plaque inflammation by enhancing drug accumulation at target sites, without compromising immunity.[3] Though several liposomally formulated anticancer drugs have already been approved for clinical use,[4] nanomedicine remains unexplored in patients with cardiovascular disease. Theoretically, an inflamed atherosclerotic plaque, characterized by endothelial dysfunction and a highly permeable microvasculature, could be an excellent target for nanomedicinal delivery.[5]

Of the numerous clinically-applied anti-inflammatory compounds, glucocorticoids (GCs) are the most widely used and have potent anti-inflammatory effects.[6] However, systemic GC treatment has not been used in patients with cardiovascular disease because long-term GC use has pro-atherogenic effects, including dyslipidemia, glucose intolerance and hypertension.[7] In contrast, locally administering GCs via drug-eluting stents has been shown to reduce neo-intimal formation and arterial wall inflammation in an experimental model.[8] These results suggest that a liposomal GC formulation may minimize systemic adverse effects while improving local anti-inflammatory efficacy. In support of this idea, we previously reported markedly reduced arterial wall inflammation following intravenous administration of liposomal prednisolone in an atherosclerotic rabbit model.[9]

Here we evaluate the clinical applicability of a long-circulating liposomal nanoparticle encapsulating prednisolone phosphate (LN-PLP) in patients with atherosclerosis. First, we determined liposomal prednisolone's pharmacokinetic profile in humans and assessed delivery to plaque macrophages isolated from iliofemoral plaques of patients referred for vascular surgery. Subsequently, we used noninvasive multimodal imaging to measure the anti-inflammatory efficacy of LN-PLP in patients with atherosclerosis.

Methods

Study participants

All participants provided written informed consent. The clinical trials were approved by the local institutional review board and conducted according to the principles of the International Conference on Harmonisation–Good Clinical Practice guidelines (Clinicaltrials.-gov registration NCT01039103, NCT01647685, NCT01601106).

Liposomal prednisolone

The liposomal nanoparticles (LNs) were composed of a hydrophilic core encapsulating prednisolone phosphate (PLP), surrounded by a lipid bilayer of phospholipids and cholesterol, which was coated with polyethylene glycol (PEG). See supplementary methods for LN-PLP formulation.

Pharmacokinetic profile of LN-PLP in humans

We conducted a single-dose escalation study, using 13subjects, to determine the pharmacokinetic performance of LN-PLP after a single intravenous (i.v.) dose of 0.375 mg/kg (n = 3), 0.75 mg/kg (n = 3) or1.5 mg/kg (n = 7)LN-PLPin a 2.5 htime frame. Serum concentrations of PL and its pro-drug PLP were measured on days 1, 3, 7 and weekly up to 12 weeks using high-performance liquid chromatography. Safety evaluation after LN-PLP administration included documenting adverse events, checking vital signs and conducing safety laboratory tests.

LN-PLP delivery in patients with iliofemoral atherosclerosis

To study LN-PLP's delivery, we performed a randomized, placebo-controlled, double-blind trial in 14 patients with iliofemoral atherosclerotic plaques who were scheduled for endarterectomy. After 1:1 randomization, patients received either 1.5 mg/kg LN-PLP (n = 7) or saline (n = 7) via an antecubital vein on days 0 and 7, followedbyvascular surgeryonday 10. The dosing regimen for LN-PLP was based on a preclinical study in rabbits[9] and adjusted according to the drug-dose conversion from rabbit to human.[10]

Plaque tissue macrophages were isolated to evaluate the presence of LN-PLP (see supplementary methods)[11]. Cells were spotted on a glass slide using a cytospin centrifuge, fixed with 0.4% paraformaldehyde (30 min), permeabilized with 0.1% Triton X-100 (10 min) and stained overnight. Primary antibodies were mouse anti-human CD68 (Abcam, Cambridge, UK; 1:100) and rabbit anti-human PEG (Epitomics, Burlingame, CA, U.S.A.; 1:100), and secondary antibodies were CyTM3-conjugated donkey anti-mouse and FITC-conjugated donkey anti-rabbit (both Jackson, West Grove, PA, 1:200). Cells were examined with fluorescence microscopy (Leica, DMRA HC Upright). Per patient, at least 4 cell spin slides were used to examine the percentage of DAPI cells positive for CD68 (macrophages) and, DAPI/CD68 cells positive for PEG (LN-PLP). A reader who was blinded for treatment allocation performed these analyses.

Local efficacy in patients with atherosclerosis

Subsequently, we evaluated LN-PLP therapeutic efficacy in a randomized, placebo-controlled, double-blind trial of 30 patients with documented history of atherosclerotic cardiovascular disease (i.e. angina pectoris, myocardial infarction, TIA or stroke). Prospective participants underwent ^{18}fluorodeoxyglucose positron emission tomography/computed tomography (FDG-PET/CT) to identify patients with marked arterial wall inflammation (TBR_{max} > 2.2, measured in either the ascending aorta or carotid arteries). Based on this criterion, five (14%) of the 36 subjects screened were not included in the study. After enrolment, patients had dynamic contrast enhanced-magnetic resonance imaging (DCE-MRI) scans of their carotid arteries prior to treatment allocation. One of the remaining 31 patients dropped out due to claustrophobia during baseline MRI acquisition. After 2:1 randomization, patients received either LN-PLP 1.5 mg/kg (n = 20) or saline (n = 10) i.v. on days 0 and 7. On day 10, we assessed therapeutic efficacy by DCE-MRI and FDG-PET/CT imaging of both carotid arteries. A blinded, experienced reader analyzed the images at the core laboratory (TMII, Department of Radiology, Mount Sinai). Prior to analysis, the image set was assessed for quality, and standard operating procedures ensured

that the same arterial segments, based on specified anatomical locations, would be analyzed by both PET/CT and (DCE)-MRI (see supplementary methods).

Statistical analysis

Baseline values and distributional characteristics are shown as mean (SD), number (frequency) or median (min–max). Independent samples t test, Mann–Whitney U test and Chi-square test were used to assess baseline differences between patients and controls. For efficacy analysis, Wilcoxon signed-rank test was used. A two-sided *P* value below 0.05 was considered statistically significant. All data were analyzed using Prism version 5.0 (GraphPad software, La Jolla, CA, USA) and SPSS version 19.0 (SPSS Inc., Chicago, IL, USA).

Results

Pharmacokinetic performance of LN-PLP in humans

Prior to investigating delivery and efficacy of LN-PLP in humans, we studied its PK profile in 13 subjects, 8 male and 5 female, with a mean age of 51 ± 10 years (Table 1). LN-PLP had a prolonged circulation half-life ($t_{½}$) ranging from 45 to 63 h. The area-under-the-curve for LN-PLP indicated a dose-dependent relationship (from 856 ± 171, 1355 ± 352, to 4135 ± 1489 μg·h/mL for 0.375, 0.75 and 1.5 mg/kg LN-PLP, respectively). The peak plasma concentration of free PL was, on average, 0.5% of the total liposomal PLP plasma concentration and remained constant throughout the 28-day experimental period (supplementary Figure S1). This constancy indicates negligible encapsulated drug leakage from the liposome into circulation, since direct leakage would accelerate PLP plasma decay and increase the percentage of free PL. Table 1 provides an overview of PK data in humans. LN-PLP was well tolerated, and no serious adverse events occurred. Further, LN-PLP did not adversely affect cardiometabolic parameters, nor did it significantly change liver and/or kidney parameters (supplementary Table S1).

Delivery of LN-PLP to plaque macrophages in patients

LN-PLP plaque delivery was evaluated in 14 patients, with a mean age of 70 ± 7 years, who were scheduled for endarterectomy due to symptomatic iliofemoral atherosclerosis. Patients were divided into two groups, one to receive LN-PLP and the other a placebo, with comparable clinical characteristics (Table 2). After surgery on day 10 post-treatment, macrophages were isolated from excised plaques and stained with DAPI (cell nuclei), CD68 (macrophages) and PEG (LN-PLP coating). In patients treated with LN-PLP, we observed a high degree of co-localization between PEG and macrophages (Figure 1, A). We observed that 88% of DAPI positive cells isolated from plaques stained positive for the macrophage marker CD68, of which 77% was also positive for liposomal PEG. As expected, CD68 positive macrophages isolated from patients treated with saline did not stain positive for PEG (Figure 1, B). This finding supports the feasibility of drug delivery to plaque macrophages in patients with atherosclerotic disease.

LN-PLP efficacy in patients with atherosclerosis

Having established feasibility, our next step was to evaluate LN-PLP's therapeutic efficacy in patients with atherosclerotic disease. At baseline, the LN-PLP and saline treatment groups had similar clinical characteristics with the exception of higher systolic blood pressure in the saline group (Table 3). After two infusions of either LN-PLP (1.5 mg/kg) or saline, local efficacy was assessed with DCE-MRI and FDG-PET/CT. In contrast to the preclinical efficacy data,[9] we did not observe a reduction in arterial wall permeability after LN-PLP treatment (Table 4). Illustrative pre- and post-treatment DCE-MRI overlay images are shown in Figure 2,A and B. The non-model-based AUC remained unaltered after two LN-PLP infusions (for the left carotid artery, 0.1143 ± 0.0619 at baseline and 0.1294 ± 0.0686 after treatment, $P = 0.45$). Accordingly, the kinetic parameter K^{trans} was not reduced by LN-PLP (for the left carotid artery, 0.1062 ± 0.0659 at baseline and 0.1259 ± 0.0651 after treatment, $P = 0.23$). The lack of change in AUC and K^{trans} was also observed in the right carotid artery (Table 4). Figure 2, C–F illustrates the DCE-MRI parameters for the left and right carotid arteries in both the LN-PLP and saline groups.

In addition, we saw no reduction in arterial wall inflammation after LN-PLP treatment (Table 4). Figure 3, A and B provides representative pre- and post-treatment CT and PET/CT images of a patient treated with LN-PLP. Treatment with LN-PLP resulted in a marginal 7% TBR_{max} increase in the left carotid artery (from 1.78 ± 0.31 at baseline to 1.90 ± 0.38 after treatment, $P = 0.03$) versusno change in patients treated with placebo (from 1.82 ±0.16 at baseline to 1.82 ± 0.24 after treatment, P = 0.16; Figure 3, C). Similarly, the TBR_{mean} increased 5% after LN-PLP infusions, whereas no change was observed in the saline treatment group (Figure 3, E). The right carotid artery demonstrated corresponding measurements, as illustrated in Fig. 3, D and F. Patients tolerated LN-PLP well, with no observed changes in vital signs or lipid, inflammatory or safety markers (supplementary Table S2).

Discussion

Our present study aimed at exploring a liposomal nanoparticle loaded with prednisolone phosphate in the clinical frontier of atherosclerotic disease. First, we show the prolonged circulation half-life of prednisolone administered as a liposomal nanoparticle in humans, making this delivery approach potentially suitable for local delivery to atherosclerotic lesions. Indeed, we observed intravenously administered liposomal prednisolone to successfully accumulate in macrophages isolated from atherosclerotic plaques of patients with symptomatic iliofemoral atherosclerosis. However, in atherosclerotic patients short-term LN-PLP treatment did not reduce arterial wall permeability or arterial wall inflammation, as assessed with multi-modal imaging. Despite the lack of anti-inflammatory efficacy, these data show, for the first time, that nanomedicinal delivery of drugs to atherosclerotic lesions is feasible in humans.

Pharmacokinetics of liposomal versus free prednisolone phosphate

Although its applications have been explored primarily in oncology, nanomedicine is a promising therapeutic approach to cardiovascular disease.[5] Efficient delivery to

atherosclerotic lesions requires preventing rapid nanoparticle removal from plasma, predominantly by the MPS. To block nanoparticle removal and allow nanoparticles to arrive at and accumulate in plaque, hydrophilic polymers, including PEG, are usually added to nanoparticle surfaces.[3] In the present study, packaging prednisolone phosphate in PEG-ylated liposomes markedly prolonged the drug's half-life to 45–63 h in humans, which is 7 to 15-fold longer than for intravenously-administrated free prednisolone phosphate.[6] These PK features will theoretically facilitate LN-PLP delivery to atherosclerotic plaques.

Delivering LN-PLP to plaque macrophages in patients

Intravenously infusing LN-PLP into the antecubital vein 10 and 3 days prior to iliofemoral endarterectomy led to LN-PLP accumulation in plaque macrophages taken from patients with symptomatic iliofemoral atherosclerosis. LNs accumulate in plaque macrophages through two possible routes. First, nanoparticles can potentially be taken up by splenic or circulating monocytes that subsequently migrate to the plaque. However, the PEG coating is designed to serve as a steric barrier that minimizes nanoparticle opsonization and uptake by phagocytic cells,[12] thus suggesting little monocyte LN uptake. Nonetheless, if circulating LNs may associate with circulating or splenic monocytes, they eventually migrate to areas of inflammation through a natural conduit,[13] as has been demonstrated in mouse models of myocardial infarction and stroke.[14] Second, LNs may extravasate due to atherosclerotic plaques' enhanced permeability, since the endothelial lining covering the atherosclerotic lesion is largely dysfunctional.[15] In addition, plaque's hypoxia-induced expansion of the vaso vasorum results in leaky neovessels with poor endothelial cell junctions.[16,17] This type of increased microvessel permeability has been shown to enhance local extravasation of long-circulating nanoparticles in cancer.[18] Thus, the increased permeability at the luminal and/or adventitial side allows for long-circulating nanoparticles to extravasate, resulting in accumulation of the LN within the subendothelial space and eventually phagocytosis by plaque macrophages. A limitation of the trial design is that we show accumulation in the iliofemoral segment but not in other atherosclerotic areas, such as the carotid arteries. This was dictated by the availability of and access to human material of patients that were allowed to enroll by the IRB. Future human studies using non-invasively traceable LN could provide more quantitative insight in LN accumulation in different anatomical locations.

Local efficacy of LN-PLP: from rabbits to patients

Whereas previously LN-PLP showed to reduce inflammation in atherosclerotic lesions in rabbits,[9] LN-PLP treatment did not induce measurable anti-inflammatory effects in the atherosclerotic artery wall in patients The discrepancy in therapeutic efficacy between the preclinical rabbit study and human trial may have several explanations.

First, it may have resulted from an insufficient dose of prednisolone reaching the plaque. Unfortunately, the present study does not allow for quantitative assessment of the concentration of prednisolone delivered to the plaque. In contrast to the previously reported 4%–10% accumulation rate of intravenously infused liposomal agents in tumors,[19] accumulation in widely-spread plaques may not have been sufficient to exert a potent anti-inflammatory effect. While increasing the LN-PLP dose will likely resolve this issue, upping the dosage may introduce the risk of adverse effects caused by high intracellular GC

concentrations. For instance, GCs have been shown to polarize macrophages towards a phenotype with a higher propensity towards lipid accumulation,[20,21] which may increase ER-stress and eventually lead to macrophage apoptosis in the plaque.[22] Moreover, GC-induced upregulation of 11β-hydroxysteroid dehydrogenase type 1 (11β-HSD1) in plaque macrophages can increase intracellular accumulation of pro-inflammatory GC.[23,24] These inadvertent negative consequences of GCs imply that, prior to increasing LN-PLP doses in patients, we should clarify intracellular GCs' impact on macrophages in the lipid-rich plaque environment.

A second reason for the lack of reduced inflammation in humans may relate to a timing issue: the trial may have been too short to detect anti-inflammatory effects. Most studies evaluating the impact of anti-inflammatory agents in human cardiovascular disease[27,28] showed therapeutic efficacy only after 12 weeks of treatment, whereas our study evaluated results after only 10 days, based on the rapid reduction in arterial wall inflammation following LN-PLP treatment in atherosclerotic rabbits. The fact that we observed an increase in arterial wall FDG uptake in patients, however, favors other factors than time contributing to the discrepant findings between rabbits and patients. In this respect, the pathobiology of rabbit and human atherosclerosis has marked differences. Atherosclerotic lesions in rabbits are induced in weeks following an acute injury response, whereas patients develop atherosclerotic plaques over the course of many decades. As a consequence, human atherosclerosis is characterized by complex plaques with a high lipid burden and a chronic low-grade inflammatory response. The observed differential therapeutic result between experimental and clinical atherosclerosis in the present study implies that the responsiveness of an acute injury reaction in the atherosclerotic rabbit model may not translate to anti-inflammatory compounds' efficacy in patients with advanced atherosclerosis.

Finally, the liposomal carrier may have had an adverse effect independent of the compound present inside the carrier, thereby masking a potential beneficial result. This scenario seems less likely, since the LNs used in our study are composed of saturated phospholipids that are inherently resistant to oxidation or pro-inflammatory effects.[25,26] In accordance with our outcomes, other phase II/III studies using PEG-ylated compounds in humans have not reported pro-inflammatory effects.[27–29] Indeed, it has been suggested that empty liposomes can regress atherosclerosis, since such particles can act as high-capacity, low-affinity acceptors of intracellular cholesterol.[30,31]

Nanomedicine-based delivery represents a new paradigm in the treatment of atherosclerotic disease.[5,32] In a first-in-human anti-atherosclerosis nanotherapy trial we demonstrated that long-circulating liposomal nanoparticles accumulate in plaque macrophages of patients. This phenomenon likely also holds true for other long-circulating nanoparticle platforms, such as micellar[33] or polymeric nanoparticles.[34] Future efforts should be aimed at the non-invasive and quantitative assessment of nanoparticle plaque targeting by imaging. This will also enable studying cardiovascular patients' heterogeneity in plaque permeability, and consequently the ability of nanoparticles to accumulate in plaques. Existing experience in rheumatoid arthritis patients with the current LN-PLP nanotherapy allowed us to accelerate its translation into cardiovascular disease. However, the GC drug payload may not have been ideal for atherosclerotic disease. Therefore, to further develop cardiovascular

nanomedicine, an important focus should be on identifying suitable drug candidates for targeted treatment of human atherosclerotic plaques with a complex inflammatory, lipid-rich micro milieu.

In conclusion, we present evidence of local delivery of intravenously administered LN-PLP into macrophages isolated from human atherosclerotic plaques. In patients with atherosclerosis, however, short-term LN-PLP administration did not achieve a significant anti-inflammatory effect in atherosclerotic lesions. Nonetheless, we emphasize the potential of nanomedicine as a novel treatment paradigm for patients with atherosclerotic disease. Our work may serve as a guide for both the development as well as efficacy readout of future antiatherosclerotic nanotherapies using imaging-assisted efficacy measures in relatively small-scaled studies.

Supplementary Material

Refer to Web version on PubMed Central for supplementary material.

Acknowledgments

Author disclosures and funding: This work was supported by a European Framework Program 7 grant (ESS, GS: FP7-Health 309820: Nano-Athero); the Dutch network for Nanotechnology NanoNext NL, in the subprogram “Drug Delivery”; the National Heart, Lung, and Blood Institute, National Institutes of Health, as a Program of Excellence in Nanotechnology (PEN) Award, Contract #HHSN268201000045C (Z.A.F.); and NIH grants R01 HL118440 (W.J.M.M.), R01 HL125703 (W.J.M.M.), R01 EB009638 (ZA.F.), andNWO Vidi 91713324 (W.J.M.M.). Additionally, this work was supported by a grant from Enceladus Pharmaceuticals (Amsterdam, The Netherlands). M.E.L was partially supported by the International Atherosclerosis Society (USA) and by the Foundation “De Drie Lichten” (The Netherlands). J.M.M. is affiliated with the company Enceladus Pharmaceuticals (Amsterdam, The Netherlands), and GS. is an advisor for the company Enceladus Pharmaceuticals (Amsterdam, The Netherlands).

Appendix A. Supplementary data

Supplementary data to this article can be found online at http://dx.doi.org/10.1016/j.nano.2015.02.021.

Abbreviations

FDG-PET/CT	^{18}fluorodeoxyglucose positron emission tomography/computer tomography
BMI	body mass index
CVD	cardiovascular disease
DCE-MRI	dynamic contrast enhanced-magnetic resonance imaging
DPPC	dipalmitoylphosphatidylcholine
DSPE	distearoylphosphatidylethano-la-mine
GC	glucocorticoids
HDL-C	high density lipoprotein cholesterol

LCA	left carotid artery
LDL-C	low density lipoprotein cholesterol
LN	liposomal nanoparticle
LN-PLP	liposomal nanoparticle encapsulating prednisolone phosphate
MPS	mononuclear phagocyte system
PEG	polyethylene glycol
PLP	prednisolone phosphate (prodrug)
PL	prednisolone (free drug)
RCA	right carotid artery
ROI	region of interest
SBP	systolic blood pressure
SUV	standardized uptake value
TBR	target to background ratio
TC	total cholesterol
TG	triglycerides
VWA	vessel wall area

References

1. Libby P, Ridker PM, Hansson GK. Progress and challenges in translating the biology of atherosclerosis. Nature. 2011; 473:317–25. [PubMed: 21593864]
2. Van der Valk FM, van Wijk DF, Stroes ESG. Novel anti-inflammatory strategies in atherosclerosis. Curr Opin Lipidol. 2012; 23:532–9. [PubMed: 23160400]
3. Wagner V, Dullaart A, Bock A-K, Zweck A. The emerging nanomedicine landscape. Nat Biotechnol. 2006; 24:1211–7. [PubMed: 17033654]
4. Zhang L, et al. Nanoparticles in medicine: therapeutic applications and developments. Transl Med. 2008; 83:761–9.
5. Lobatto ME, Fuster V, Fayad ZA, Mulder WJM. Perspectives and opportunities for nanomedicine in the management of atherosclerosis. Nat Rev Drug Discov. 2011; 10:835–52. [PubMed: 22015921]
6. Czock D, Keller F, Rasche FM, Häussler U. Pharmacokinetics and pharmacodynamics of systemically administered glucocorticoids. Clin Pharmacokinet. 2005; 44:61–98. [PubMed: 15634032]
7. Wei L. Taking glucocorticoids by prescription is associated with subsequent cardiovascular disease. Ann Intern Med. 2004; 141:764. [PubMed: 15545676]
8. Wang L, et al. Stent-mediated methylprednisolone delivery reduces macrophage contents and in-stent neointimal formation. Coron Artery Dis. 2005; 16:237–43. [PubMed: 15915076]
9. Lobatto ME, et al. Multimodal clinical imaging to longitudinally assess a nanomedical anti-inflammatory treatment in experimental atherosclerosis. Mol Pharm. 2010; 7:2020–9. [PubMed: 21028895]
10. Reagan-Shaw S, Nihal M, Ahmad N. Dose translation from animal to human studies revisited. FASEB J. 2008; 22:659–61. [PubMed: 17942826]

11. Allen TM, Cullis PR. Drug delivery systems: entering the mainstream. Science. 2004; 303:1818–22. [PubMed: 15031496]
12. Hak S, et al. The effect of nanoparticle polyethylene glycol surface density on ligand-directed tumor targeting studied in vivo by dual modality imaging. ACS Nano. 2012; 6:5648–58. [PubMed: 22671719]
13. Swirski FK, Nahrendorf M. Leukocyte behavior in atherosclerosis, myocardial infarction, and heart failure. Science. 2013; 339:161–6. [PubMed: 23307733]
14. Flögel U, et al. In vivo monitoring of inflammation after cardiac and cerebral ischemia by fluorine magnetic resonance imaging. Circulation. 2008; 118:140–8. [PubMed: 18574049]
15. Davignon J, Ganz P. Role of endothelial dysfunction in atherosclerosis. Circulation. 2004; 109:III27–32. [PubMed: 15198963]
16. Virmani R, et al. Atherosclerotic plaque progression and vulnerability to rupture: angiogenesis as a source of intraplaque hemorrhage. Arterioscler Thromb Vasc Biol. 2005; 25:2054–61. [PubMed: 16037567]
17. Ritman EL, Lerman A. The dynamic vasa vasorum. Cardiovasc Res. 2007; 75:649–58. [PubMed: 17631284]
18. Lammers T, Kiessling F, Hennink WE, Storm G. Drug targeting to tumors: principles, pitfalls and (pre-) clinical progress. J Control Release. 2012; 161:175–87. [PubMed: 21945285]
19. Bartlett DW, Su H, Hildebrandt IJ, Weber WA, Davis ME. Impact of tumor-specific targeting on the biodistribution and efficacy of siRNA nanoparticles measured by multimodality in vivo imaging. Proc Natl Acad Sci U S A. 2007; 104:15549–54. [PubMed: 17875985]
20. Liew YY, Docter E, Ray DW, Hutchinson IV, Brogan IJ, Docter E, Ray DW, Hutchinson IV, Brogan IJ. Effect of rapamycin and prednisolone in differentiated THP-1 and U937 cells. Transplant Proc. 2002; 34:2872–3. [PubMed: 12431638]
21. Hu W, et al. Statins synergize dexamethasone-induced adipocyte fatty acid binding protein expression in macrophages. Atherosclerosis. 2012; 222:434–43. [PubMed: 22503826]
22. Spann NJ, et al. Regulated accumulation of desmosterol integrates macrophage lipid metabolism and inflammatory responses. Cell. 2012; 151:138–52. [PubMed: 23021221]
23. Luo MJ, et al. 11 β-HSD1 inhibition reduces atherosclerosis in mice by altering pro-inflammatory gene expression in the vasculature. Physiol Genomics. 2012; 7:47–57. [PubMed: 23170035]
24. Hadoke PWF, Kipari T, Seckl JR, Chapman KE. Modulation of 11β-hydroxysteroid dehydrogenase as a strategy to reduce vascular inflammation. Curr Atheroscler Rep. 2013; 15:320. [PubMed: 23512604]
25. Alipour M, et al. Safety and pharmacokinetic studies of liposomal antioxidant formulations containing N-acetylcysteine, α-tocopherol or γ-tocopherol in beagle dogs. Toxicol Mech Methods. 2013; 23:419–31. [PubMed: 23384394]
26. Mamidi RNVS, et al. Pharmacokinetics, efficacy and toxicity of different pegylated liposomal doxorubicin formulations in preclinical models: is a conventional bioequivalence approach sufficient to ensure therapeutic equivalence of pegylated liposomal doxorubicin products? Cancer Chemother Pharmacol. 2010; 66:1173–84. [PubMed: 20661737]
27. Musacchio T, Torchilin V. Recent developments in lipid-based pharmaceutical nanocarriers. Front Biosci. 2011; 16:1388–412.
28. Torchilin VP. Recent advances with liposomes as pharmaceutical carriers. Nat Rev Drug Discov. 2005; 4:145–60. [PubMed: 15688077]
29. Metselaar JM. Liposomal targeting of glucocorticoids to synovial lining cells strongly increases therapeutic benefit in collagen type II arthritis. Ann Rheum Dis. 2004; 63:348–53. [PubMed: 15020326]
30. Dass CR, Jessup W. Apolipoprotein A-I, cyclodextrins and liposomes as potential drugs for the reversal of atherosclerosis. A review. J Pharm Pharmacol. 2000; 52:731–61. [PubMed: 10933125]
31. Rodrigueza WV, Klimuk SK, Pritchard PH, Hope MJ. Cholesterol mobilization and regression of atheroma in cholesterol-fed rabbits induced by large unilamellar vesicles. Biochim Biophys Acta. 1998; 1368:306–20. [PubMed: 9459607]
32. Mulder WJM, Jaffer FA, Fayad ZA, Nahrendorf M. Imaging and nanomedicine in inflammatory atherosclerosis. Sci Transl Med. 2014; 6:239.

33. Torchilin VP. Micellar nanocarriers: pharmaceutical perspectives. Pharm Res. 2007; 24:1–16. [PubMed: 17109211]

34. Pridgen EM, Langer R, Farokhzad OC. Biodegradable, polymeric nanoparticle delivery systems for cancer therapy. Nanomedicine (Lond). 2007; 2:669–80. [PubMed: 17976029]

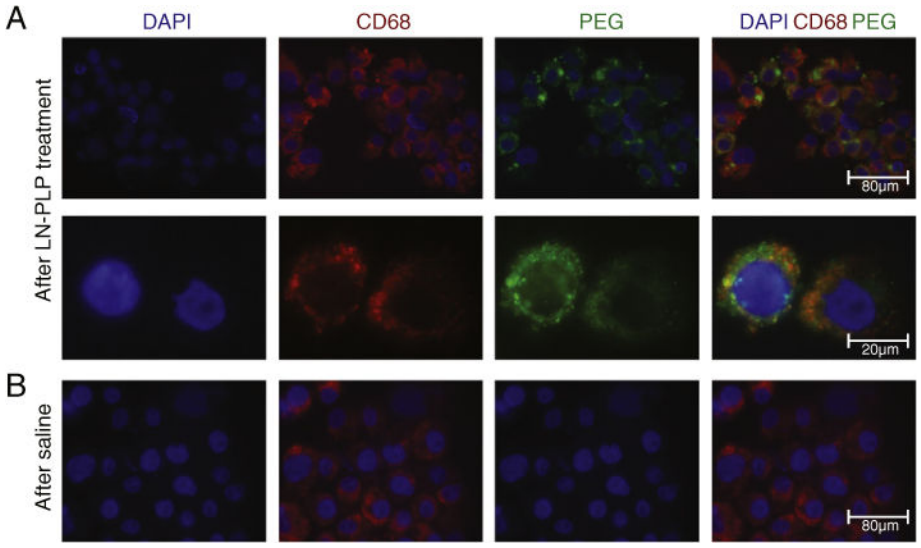

Figure 1.

Local accumulation of LN-PLP in macrophages of iliofemoral plaques. **(A)** Microscopic images of cells isolated from a plaque of a patient treated with LN-PLP stained for cell nuclei (DAPI) and macrophages (CD68) and the liposome-coating polyethylene glycol (PEG). Below, the enlargement of two cells corroborates the co-localization of CD68 cells and PEG. **(B)** Microscopic images illustrating that CD68 positive cells isolated from a plaque of a patient treated with saline do not show positivity for PEG.

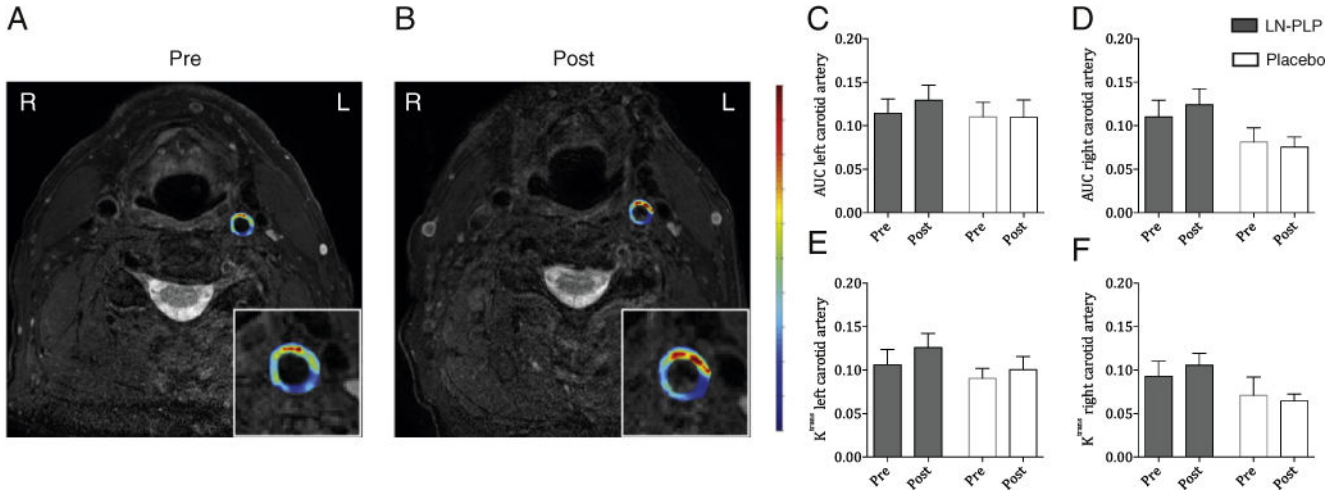

Figure 2.

Arterial wall permeability after LN-PLP infusion in patients. **(A–B)** Representative axial T1-weighted MR images of the carotid arteries; the inset shows a magnification of the left carotid artery with a superimposed AUC map before and after LN-PLP treatment. **(C–F)** Bar graphs demonstrating the lack of reduction in AUC and K^{trans} for the left carotid artery **(C–D)** and right carotid artery **(E–F)**.

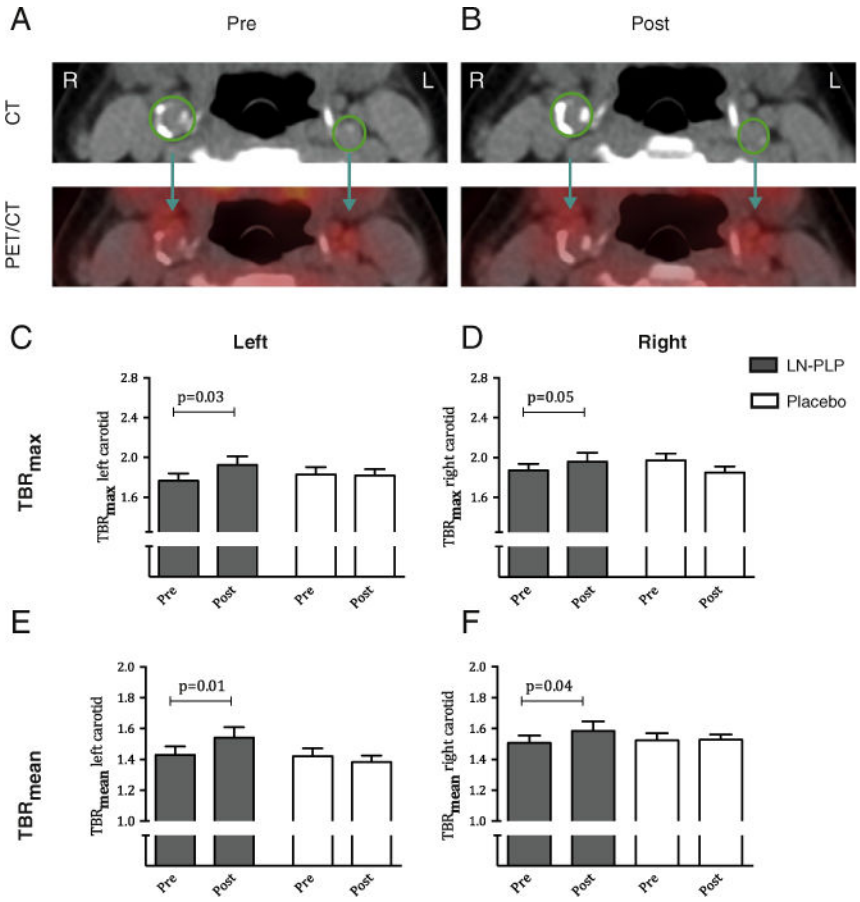

Figure 3.

Arterial wall inflammation after LN-PLP infusion in patients. **(A–B)** Representative axial computed tomography (CT) and positron emission tomography (PET)/CT images of the carotid arteries before and after LN-PLP treatment, with region of interest (ROI) shown in green. **(C–F)** Bar graphs showing the change in TBR_{max} and TBR_{mean} in the left carotid artery **(C–D)** and right carotid artery **(E–F)**.

Table 1

Pharmacokinetic properties of LN-PLP in humans.

Clinical characteristics	0.375 mg/kg (n = 3)	0.75 mg/kg (n = 3)	1.5 mg/kg (n = 7)
Age (years)	53 ± 12	44 ± 5	57 ± 12
Gender (male%)	2 (67)	2 (67)	4 (57)
PK parameters			
AUC (0–168 h) (μg·ml·h^{-1})	856 ± 171	1355 ± 352	4135 ± 1489
t½ (h)	45.0 ± 26.0	42.7 ± 12.8	62.5 ± 11.9
CL (L/h)	0.041 ± 0.011	0.054 ± 0.016	0.031 ± 0.010
PL/PLP ratio	0.55	0.65	0.41

AUC = Area under the concentration curve; t½ = half-life; CL = plasma clearance; Vss = volume of distribution at steady state; PL/PLP ratio = proportion free prednisolone of total liposomal prednisolone phosphate. Data are presented as mean ± SD.

Table 2

Clinical characteristics of patients in the nanomedicine delivery study.

Clinical characteristic	LN-PLP (n = 7)	Placebo (n = 7)
Age	67 ± 5.9	73 ± 7.8
Gender, *male n (%)*	7 (100%)	6 (86%)
BMI, kg/m^2	27.3 ± 5.0	26.0 ± 5.2
SBP, *mmHg*	130 ± 8.0	136 ± 10.0
Lipid profile:		
Total cholesterol, *mmol/L*	4.4 ±1.1	4.0 ± 1.0
LDLc, *mmol/L*	2.3 ± 0.6	2.1 ± 0.5
HDLc, *mmol/L*	1.1 ± 0.4	1.2 ± 0.4
TG, *mmol/L*	2.0 ± 1.1	2.1 ± 1.0

BMI = body mass index; SBP = systolic blood pressure; LDLc = low density lipid cholesterol; HDLc = high density lipid cholesterol; TG = triglycerides. Data are presented as mean ± SD or number (percentage).

Table 3

Clinical characteristics in the efficacy study.

	LN-PLP (n = 20)	Placebo (n = 10)
Inclusion parameters		
TBR_{max} AA	2.80 ± 0.42	2.81 ± 0.42
TBR_{max} LCA	1.78 ± 0.31	1.83 ± 0.24
TBR_{max} RCA	1.87 ± 0.28	1.97 ± 0.22
Baseline characteristics		
Age	61 ± 7	59 ± 7
Gender, *m (m %)*	16 (80%)	8 (80%)
BMI, kg/m^2	29.0 ± 4.5	28.4 ± 3.5
SBP, *mmHg*	130 ± 13*	150 ± 13*
Lipid profile		
Total *cholesterol, mmol/L*	5.86 ± 2.30	5.63 ± 1.71
LDLc, *mmol/L*	3.96 ± 2.31	3.92 ± 1.53
HDLc, *mmol/L*	1.33 ± 0.50	1.09 ± 0.45
TG, *mmol/L*	1.51 ± 1.10	1.56 ± 0.81

AA = ascending aorta; BMI = body mass index; SBP = systolic blood pressure; LCA = left carotid artery; LDLc = low density lipid cholesterol; HDLc = high density lipid cholesterol; RCA = right carotid artery; TG = triglycerides. Data are presented as mean ± SD or number (percentage),

* $P < 0.05$.

Table 4

DCE-MRI and PET/CT imaging at baseline and after treatment.

		LN-PLP (n = 20)			Placebo (n = 10)		
		Pre	**Post**	***P* value**	**Pre**	**Post**	***P* value**
DCE-MRI							
LCA	AUC	0.1143 ± 0.0619	0.1294 ± 0.0686	0.45	0.1103 ± 0.0472	0.1095 ± 0.0633	0.48
	K^{trans}	0.1062 ± 0.0659	0.1259 ± 0.0651	0.23	0.0904 ± 0.0323	0.1005 ± 0.0475	0.25
RCA	AUC	0.1061 ± 0.0712	0.1195 ± 0.0732	0.48	0.0821 ± 0.0455	0.0760 ± 0.0360	0.89
	K^{trans}	0.0929 ± 0.0673	0.1058 ± 0.0542	0.09	0.0798 ± 0.0613	0.0646 ± 0.0255	0.55
PET/CT							
LCA	TBR_{max}	1.78 ± 0.31	1.90 ± 0.38	*0.03*	1.82 ± 0.16	1.82 ± 0.24	0.16
	TBR_{mean}	1.43 ± 0.23	1.54 ± 0.29	*0.01*	1.42 ± 0.16	1.38 ± 0.14	0.39
RCA	TBR_{max}	1.87 ± 0.28	1.96 ± 0.38	*0.05*	1.86 ± 0.22	1.85 ± 0.20	0.07
	TBR_{mean}	1.51 ± 0.20	1.58 ± 0.26	*0.04*	1.57 ± 0.15	1.56 ± 0.17	0.86

AUC = area under the curve; DCE-MRI = dynamic contrast enhanced-magnetic resonance imaging; LCA = left carotid artery; PET/CT = positron emission tomography-computer tomography; RCA = right carotid artery; TBR = target-to-background-ratio. Data are presented as mean ± SD.